ACS APPLIED MATERIALS & INTERFACES

Research Article

www.acsami.org

Effect of Polyelectrolyte Electron Collection Layer Counteranion on the Properties of Polymer Solar Cells

Thu Trang Do,[†] Hee Seob Hong,[†] Ye Eun Ha,[†] Juyun Park,[‡] Yong-Cheol Kang,[‡] and Joo Hyun Kim*[,†]

[†]Department of Polymer Engineering, Pukyong National University, Busan 608-739, Korea

[‡]Department of Chemistry, Pukyong National University, Busan 608-737, Korea

Supporting Information

ABSTRACT: Polyviologen (PV) derivatives are known materials used for adjusting the work function (WF) of cathodes by reducing the electron injection/collection barrier at the cathode interface. To tune and improve device performance, we introduce different types of counteranions (CAs), such as bromide, tetrafluoroborate, and tetraphenylborate, to a PV derivative. The effective WF of the Al cathode is shown to depend on the size of the CA, indicating that a Schottky barrier can be modulated by the size of the CA. Through the increased size of the CA from bromide to tetraphenylborate, the effective WF of the Al cathode is gradually decreased, indicating a decreased Schottky barrier at the cathode interface. In addition, the change of the power conversion efficiency (PCE) and the short circuit current (J_{sc}) value show good correlation with the change of the WF of the cathode, signifying the typical transition from a Schottky to an Ohmic contact. The turn-on electric field of the electron-only device without PV was 0.21 MV/cm, which is dramatically higher than those of devices with PV-X (0.07 MV/cm for PV-Br, 0.06 MV/cm for PV-BF_4, and 0.05 MV/cm for PV-BPh_4) This is also coincident with a decrease in the Schottky barrier at the cathode interface. The device ITO/PEDOT/P3HT:PCBM/PV/Al, with a thin layer of PV derivative and tetraphenylborate CA as the cathode buffer layer, has the highest PCE of 4.02%, an open circuit voltage of 0.64 V, a J_{sc} of 11.6 mA/cm^2, and a fill factor of 53.0%. Our results show that it is possible to improve the performance of polymer solar cells by choosing different types of CAs in PV derivatives without complicated synthesis and to refine the electron injection/collection barrier height at the cathode interface.

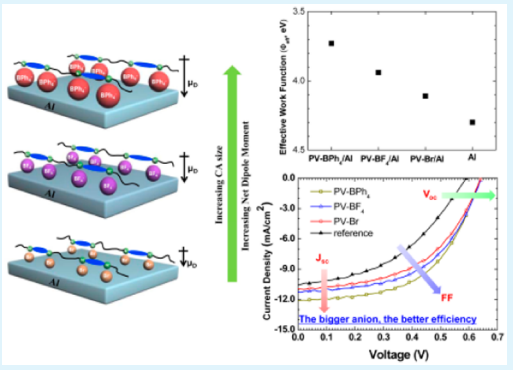

KEYWORDS: *polyelectrolyte, anion exchange, polymer solar cell, buffer layer*

INTRODUCTION

Recently, polymer solar cells (PSCs) have attracted attention because of their possible application in energy harvesting devices due to their flexibility and low fabrication cost.[1−3] Photoinduced charge separation, transportation, and collection properties are very important factors for the construction of efficient PSCs. Among them, charge carrier injecting/collecting properties are crucial for improving the performance of the devices, which are strongly related to the interfacial properties between the organic semiconducting layer and the cathode (or anode). The interfacial property at the cathode interface is improved simply by the insertion of solution processable conjugated polymer electrolytes (CPEs),[4−11] alcohol soluble neutral conjugated polymers,[12,13] polyviologen (PV) derivatives,[14] nonconjugated polymer electrolytes,[15,16] and nonconjugated polymers with polar groups, such as poly(vinylpyrrolidone),[17] poly(ethylene oxide),[18] and poly(vinyl alcohol).[19] These materials enable the fabrication of a multilayer device without destroying a precoated organic semiconducting layer because they are soluble in polar solvents (e.g., water, alcohol, etc.). Through the insertion of a thin layer of these materials at the cathode interface, the performance of PSCs is dramatically improved relative to that of devices lacking these materials as an interfacial layer.

Park et al.[20] reported that spontaneous organization of CPEs occurs during the spin coating process. Ionic components of the CPE accumulate at the top of the CPE surface because the hydrophobic semiconducting polymer layer rejects the ionic groups. Thus, the ionic or polar groups of interfacial materials can help the electric fields redistribute within a device and allow them to show permanent dipoles via their spontaneous orientation on top of either a hydrophobic organic active layer or a hydrophilic metal electrode (i.e., cathode). Therefore, it is possible to refine the energy barrier for the electron injection/collection at the cathode interface through the formation of favorable interface dipoles. If these ionic or polar materials are placed at the cathode interface, the work function (WF) of the cathode can be modified, and the energy barrier between the organic semiconducting layer and the cathode can be reduced. The presence of counteranions (CAs) in CPE structures provides another simple way of fine-tuning

Received: November 24, 2014
Accepted: January 22, 2015
Published: January 22, 2015

DOI: 10.1021/am5082606
ACS Appl. Mater. Interfaces 2015, 7, 3335−3341

Scheme 1. Synthesis and Chemical Structure of PV Derivatives with Different Types of CAs

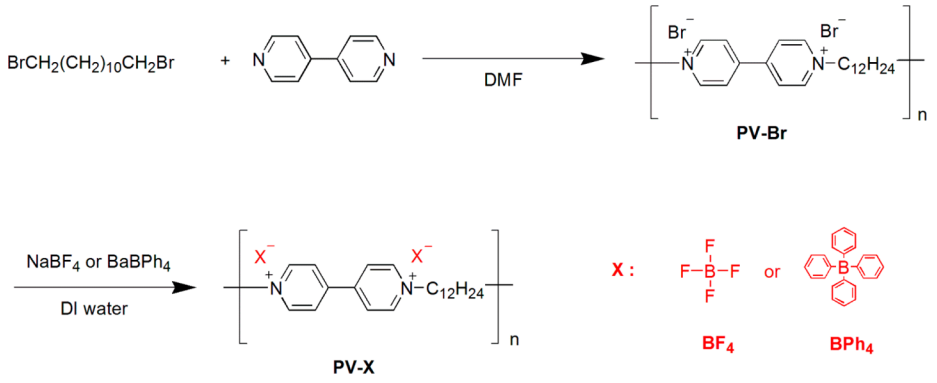

the properties of the interface by using different types of CAs.[21−25] Moreover, the WF of the electrodes, such as indium tin oxide (ITO) and Au, can be simply tuned by altering the ion density[26] and the type of CA[27] in the CPE.

PV derivatives[14] have been reported as an interfacial layer material to improve the performances of both conventional and inverted PSCs through the formation of favorable interface dipoles at the cathode interface, which reduces the electron injection/collection barrier from the active layer to the cathode. To the best of our knowledge, the effects of different CAs in CPEs or polyelectrolytes as a cathode buffer layer on photovoltaic properties have not been carefully investigated.[24] Thus, we introduced a cationic PV derivative to different types of CAs (Scheme 1), such as bromide (Br^-), tetrafluoroborate (BF_4^-), and tetraphenylborate (BPh_4^-), and carefully investigated the effect of CA size in a PV derivative acting as a cathode buffer layer on the performance of PSCs with the structure ITO/PEDOT/P3HT:PCBM/PV-X/Al (X denotes CA). We refer to PV derivatives with bromide, tetrafluoroborate, and tetraphenylborate as PV-Br, PV-BF_4, and PV-BPh_4, respectively. The van der Waals radii of the CAs[28] are ordered such that Br^- (0.19 nm) < BF_4^- (0.23 nm) < BPh_4^- (0.42 nm). Basically, the dipole moment of the compound comprising two point charges is proportional to the distance between the two charges such that the dipole moment of the thin layer of PV derivatives on the cathode will be in the order PV-Br < PV-BF_4 < PV-BPh_4. We found that the WF effect of Al electrodes with a very thin layer of PV-X is dependent on the size of the CA, indicating that a larger CA leads to a larger interface dipole (i.e., a larger reduction in the effective WF). As a result, the device with a thin layer of PV-BPh_4 as the cathode buffer layer showed the best power conversion efficiency (PCE) of 4.02% and had an open circuit voltage (V_{oc}) of 0.64 V, a short circuit current density (J_{sc}) of 11.6 mA/cm^2, and a fill factor (FF) of 53.0%.

EXPERIMENTAL SECTION

Materials. Chemicals were purchased from Aldrich Chemical Co. and Alfa Aesar and were used as received unless otherwise described. Regioregular poly(3-hexylthiophene-2,5-diyl) (P3HT, No. 4002-EE) and phenyl C_n butyric acid methyl ester (PCBM, No. nano-cPCBM-BF) were purchased from Rieke Metals, Inc. and Nano-C, Inc., respectively.

Poly(1,1′-didodecyl-4,4′-bipyridinium dibromide) (PV-Br). PV-Br was synthesized according to procedures in the litereature (Scheme 1).[14] A yellowish brown solid was recoverd with 86.8% yield (1.26 g). ^{1}H NMR (400 MHz, CD_3OD): δ 9.15−9.12 (br, 4H), 8.59−8.56 (br, 4H), 4.77−4.72 (br, N^+-CH_2-, 4H), 2.15−2.06 (br, -CH_2-, 4H), 1.42−1.26 (br, -CH_2-, 16H). ^{13}C NMR (100 MHz, D2O): δ 151.12, 146.61, 128.18, 63.46, 31.80, 29.78, 29.67, 29.28, 26.47. Anal. Calcd for $C_{22}H_{33}Br_2N_2$: C, 54.45; H, 6.85; N, 5.77; Br, 32.93. Found: C, 56.93; H, 7.45; N, 5.31.

General Anion Exchange Reaction Procedure . A portion of 0.520 mmol of anion in 5 mL of deionized water (DI water, ∼18 MΩ cm) was added dropwise to a solution of PV-Br (61.0 mg, 0.130 mmol) in 5 mL of DI water. The reaction mixture was stirred at room temperature for 24 h. Precipitates were collected by filtration, washed with a copious amount of DI water (50 mL), and dried under a vacuum.

Poly(1,1′-didodecyl-4,4′-bipyridinium ditetrafluoroborate) (PV-BF_4). PV-BF_4 was obtained by an anion exchange reaction between 61.0 mg (0.130 mmol) of PV-Br and 58.0 mg (0.520 mmol) of sodium tetrafluoroborate through the general procedure. The yield was 90.1% (60.0 mg). ^{1}H NMR (400 MHz, DMSO-d_6): δ 9.38 (br, 4H), 8.78 (br, 4H), 4.67 (br, N^+-CH_2-, 4H), 1.98 (br, -CH_2-, 4H), 1.32−1.28 (br, -CH_2-, 16H). Anal. Calcd for $C_{22}H_{33}B_2F_8N_2$: C, 52.94; H, 6.66; N, 5.61; B, 4.33; F, 30.45. Found: C, 53.21; H, 6.73; N, 5.48.

Poly(1,1′-didodecyl-4,4′-bipyridinium ditetraphenylborate) (PV-BPh_4). PV-BPh_4 was prepared by an anion exchange reaction between 61.0 mg (0.130 mmol) of PV-Br and 180.0 mg (0.520 mmol) of sodium tetraphenylborate through the general procedure. The yield was 88.4% (113 mg). ^{1}H NMR (400 MHz, DMSO-d_6): δ 9.32−9.27 (br, 4H), 8.65−8.60 (br, 4H), 7.17 (br, 8H), 6.93−6.89 (t, J = 8.0 Hz, 8H), 6.79−6.75 (t, J = 8.0 Hz, 4H), 4.60 (br, N^+-CH_2-, 4H), 1.92 (br, -CH_2-, 4H), 1.29−1.24 (br, -CH_2-, 16H). Anal. Calcd for $C_{70}H_{73}B_2N_2$: C, 87.22; H, 7.63; N, 2.91; B, 2.24. Found: C, 87.51; H, 7.33; N, 3.02.

Measurements. The film thickness was measured by an Alpha-Step IQ surface profiler (KLA-Tencor). The work function measurements were carried out using ultraviolet photoelectron spectroscopy (UPS) (VG Scientific) with a He I source ($h\nu$ = 21.2 eV) at a pressure of 1 × 10^{-8} Torr. Avoltage of −3 V was applied to a sample during the measurements to distinguish between the analyzer and sample cutoff. Kelvin probe microscopy (KPM) measurements (model KP020, KP Technology, Ltd.) were performed to confirm the work function of a bare Al and PV-X-coated Al surface, which are estimated by the contact potential difference between the sample and the KP tip. The KP tip work function was calibrated by standard gold with a work function of 5.1 eV. A thin PV layer (∼5 nm) was spin coated from solution in a dimethylsulfoxide (DMSO) and methanol (MeOH) mixed solvent (5:95 DMSO/MeOH by volume) on a 100 nm thick Al/glass plate under ambient conditions for UPS and KPM measurements. The current density−voltage measurements under 1.0 sun (100 mW/cm^2) from a 150 W Xe lamp with an air mass (AM) 1.5G filter were performed using a KEITHLEY model 2400 source-measure unit. A calibrated Si reference cell with a KG5 filter certified by the National Institute of Advanced Industrial Science and Technology was used to confirm the 1.0 sun condition.

Fabrication of PSCs. For the fabrication of conventional-type PSCs with an ITO/PEDOT/active layer (P3HT:PCBM)/PV structure or without PV-X/Al, 40 nm thick PEDOT:PSS (Baytron P, diluted with 2-propanol to 1:2 v/v) was spin coated on a precleaned

DOI: 10.1021/am5082606
ACS Appl. Mater. Interfaces 2015, 7, 3335−3341

ITO glass substrate (sheet resistance = 15 Ω/sq). After being baked at 150 °C for 10 min under air, the active layer was spin cast from a blended solution of P3HT and PCBM (20 mg of each P3HT and PCBM dissolved in 1 mL of *o*-dichlorobenzene (ODCB)) at 600 rpm for 40 s and then dried in a covered Petri dish for 1 h. Prior to spin coating, the active solution was filtered through a 0.45 μm membrane filter. The typical thickness of the active layer was 200 nm. Before cathode deposition, the cathode buffer layer of PV derivatives was prepared by spin coating from solution in a DMSO and MeOH mixed solvent (5:95 DMSO/MeOH by volume) onto the active layer. The typical thickness of the cathode buffer layer was less than 5 nm. The Al layer was deposited with a thickness of 100 nm through a shadow mask with a device area of 0.13 cm^2 at 2 × 10^{-6} Torr. After the cathode was deposited, the device was thermally annealed at 150 °C for 10 min in a glovebox under a N_2 atmosphere.

Fabrication of Electron-Only Devices. An ∼70 nm thick PCBM layer was spin cast from the solution in chloroform on a precleaned ITO glass substrate (sheet resistance = 8 Ω/sq). Prior to spin coating, the PCBM solution was filtered through a 0.20 μm membrane filter. Deposition of the cathode buffer layer (∼5 nm) onto the PCBM layer was followed by preparation of the polymer solar cells. The Al layer was deposited with a thickness of 100 nm through a shadow mask with a device area of 0.09 cm^2. Current density relative to electric field curves were recorded using a KEITHLEY model 2400 source-measure unit.

RESULTS AND DISCUSSION

Synthesis and Characterization of PV Derivatives. PV derivatives with different types of CAs (Scheme 1) were obtained by a simple ion exchange reaction between PV-Br and an excess of salt with the CA of interest. The precipitates were filtered and washed with a copious amount of DI water until the bromide was removed. The chemical structure of PV-X (PV derivatives with different CAs (X)) was confirmed by X-ray photoelectron spectroscopy (XPS). As shown in Figure 1(a), PV-Br shows characteristic peaks of bromide at binding energies (BEs) of 65.3, 178.5, 185.5, and 252.5 eV, which correspond to Br3d, Br3p3/2, Br3p1/2, and Br3s, respectively. As shown in the XPS spectra of PV-BF_4 and PV-BPh_4, the bromide peaks completely disappear, and peaks at BEs of 29 and 683.5 eV were observed, which are characteristics of F1s and F2s, respectively. In addition, a tiny peak at a BE of 192 eV (boron) was observed in the XPS spectrum of PV-BF_4. Moreover, we confirmed the chemical structure of PV-X by ^{1}H NMR spectra (Figure 1(b)). The chemical shifts of protons at the 2- and 6-positions of two pyridinium rings (H_a and H_b) appeared near 9.1 and 8.5 ppm, respectively, for PV-Br. The chemical shifts of protons on pyridinium rings in PV-BF_4 and PV-BPh_4 are shifted downfield because of the CA and appear at 9.4 and 8.6 ppm, respectively. In addition, peaks appeared at 7.2−6.7 ppm, which correspond to the chemical shift of the protons in BPh_4^-. The number-average molecular weight (M_n) of PV-Br estimated from the relative peak area ratio of H_a and a peak at 4.2 ppm was 27480 Da. A chemical shift at 4.2 ppm corresponds to methylene protons at the end group.

Investigation of the Effective WF of the Al Electrode Covered with PVs. As illustrated in Figure 2(a), it is known that the effective WF (Φ_{eff}) of metal can be refined by introducing a thin layer of PV derivatives.[14] This is due to the formation of a favorable dipole at the interface. To understand how the Φ_{eff} of Al is affected by the thin film of PVs with different types of CAs, we performed an ultraviolet photoelectron spectroscopy (UPS) experiment, which is well-known as a powerful instrument for investigating the WF and vacuum level shift at the buffer layer/metal interface. The WF is

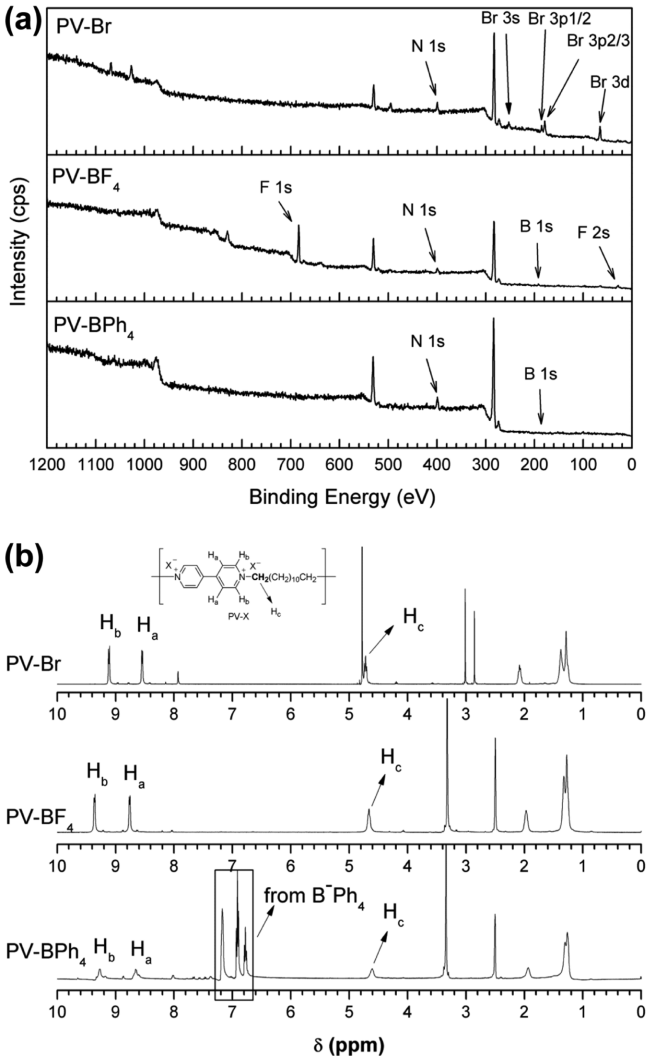

Figure 1. (a) XPS and (b) ^{1}H NMR spectra of PV derivatives with different types of CAs.

estimated from the cutoff energy and the Fermi edge.[14−16,19,29,30] As shown in Figure 2(b), the estimated WF of Al was 4.3 eV. The Φ_{eff} values of PV-Br-, PV-BF_4-, and PV-BPh_4-coated Al were 4.11, 3.94, and 3.73 eV, respectively, which are smaller than that of bare Al. As summarized in Figure 2(c), the change in the Φ_{eff} of Al covered with PV-X correlated well with the size of the CA in the PV derivative. Figure 3 presents a schematic illustration of the arrangement of the PV backbone with a CA near the surface of an Al electrode. The ordering of a CA and the PV backbone must be very complicated in the bulk state; however, the CA of PV derivatives would be directed toward the Al surface in a few layers of PV derivatives as illustrated in Figure 3. Larger CAs lead to a larger interface dipole (i.e., a larger reduction in the Φ_{eff} (Figure 3)). The Φ_{eff} of Al covered with PV-BPh_4 is almost 0.6 eV smaller than that of bare Al. Seo et al.[21] reported that comparing the properties of CPEs shows how critical properties of the semiconducting component can be modified by the choice of CA. They showed that a larger CA leads to a larger interface dipole, a more pronounced band bending at the interface between the Au electrode and the thin layer of CPEs, and a smaller Φ_{eff} of the Au cathode. From these results, the Φ_{eff} of the Al electrode is also observed to decrease gradually

DOI: 10.1021/am5082606
ACS Appl. Mater. Interfaces 2015, 7, 3335−3341

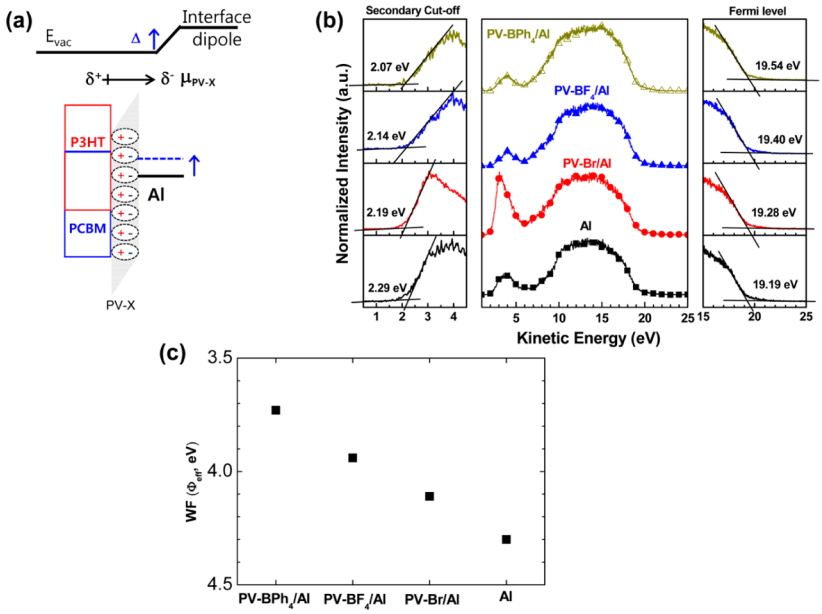

Figure 2. (a) Proposed WF reduction by the formation of interface dipoles at the surface of the cathode (Δ, work function reduction), (b) UPS spectra of PV-BPh_4-coated Al (open triangle), PV-BF_4-coated Al (filled triangle), PV-Br-coated Al (circle), and bare Al (square), and (c) the Φ_{eff} (estimated from the cutoff energy and the Fermi edge) vs PV-X-coated and bare Al.

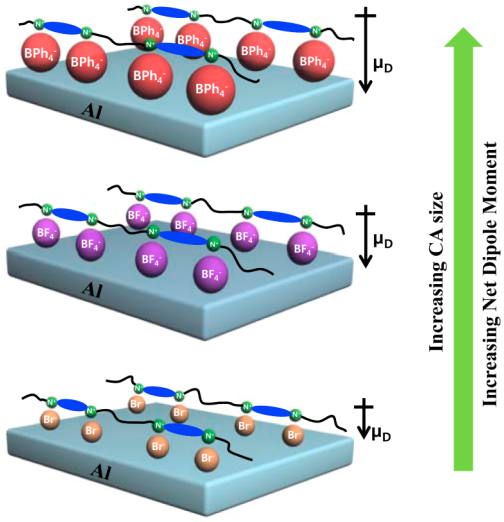

Figure 3. Proposed configuration of the CA near the surface of the Al electrode and the size dependence of a net dipole moment of PV-X (μ_D, net dipole moment at the interface).

upon increasing the size of the CA. Figure 3 shows a schematic illustration of the proposed configuration of the CA orientation on the surface of the Al electrode and the change in the magnitude of the interface dipole upon changing the CA. To crosscheck the Φ_{eff} variation by the PV thin film, we measured the Φ_{eff} by KPM analysis. The Φ_{eff} values of thin layer PV-Br-, PV-BF4-, and PV-BPF4-coated Al were 4.23 ± 0.02, 4.17 ± 0.03, and 4.01 ± 0.02 eV, respectively, which are smaller than that of bare Al (4.35 ± 0.02 eV). The KPM results also support the notion that the Φ_{eff} of the Al cathode is reduced by the formation of an interface dipole, and that the size of the CA affects the Al Φ_{eff}.

Photovoltaic Properties of Polymer Solar Cells with PV Derivatives with Different Types of CAs. To investigate the influence of the Φ_{eff} of the Al cathode on photovoltaic properties, we fabricated conventional-type PSCs with PV-X as the cathode buffer layer with a structure of ITO/PEDOT:PSS/active layer (P3HT:PCBM)/PV-X/Al. The V_{oc} values (Figure 4(a) and Table 1) of the devices with PV-X were 0.64 V, which is slightly higher (50 mV) than that of the reference device (0.59 V). This is due to the formation of favorable interface dipoles directed toward the Al cathode. As shown in the current density−voltage curve under dark conditions (inset of Figure 4(a)), the dark currents of the devices with interlayers were slightly suppressed. This indicates increased V_{oc}, which can be understood from the physics of V_{oc} in p−n junction solar cells.[31−33] However, the V_{oc} value of the device with PV derivatives does not seem to be affected by the Φ_{eff} of the Al electrodes. This is presumably due to the leakage current of the devices with interlayers (inset of Figure 4(a)) being almost the same. Here, we found that V_{oc} enhancement for the device with interlayers was not sensitive to the PV derivatives and that enhancement was up to 50 mV.

A schematic energy diagram of the devices and the Φ_{eff} of the Al electrode with different PV derivatives are shown in Figure 4(b). The WF reduction of the Al cathode by the thin layer of PV derivatives results in an energy difference between the WF of the cathode and the WF of the ITO/PEDOT that is increased, indicating that the internal electric field in the device is larger than that of the device without PV derivatives. Thus, the collection of electrons from the active layer to the Al cathode under the short circuit condition will be more efficient. This is one reason the device with PV derivatives has a J_{sc} that is higher than that of the reference device. Here, the improved PCE of the device with PV-Br over the PCE of the device from our previous report[14] seems to be due to processing solvent for PV-Br. One possible reason for the inferior performance is the film-forming quality of PV-Br on the active layer from its solution in 5:95 DMSO/methanol, which may may be better than that of the solution in 30:70 water/isopropanol. It is commonly known that the solvent for the buffer layer is a critical factor for film-forming properties.[14,19] As shown in Table 1, the PCEs of the devices with PV-Br, PV-BF_4, and PV-

DOI: 10.1021/am5082606
ACS Appl. Mater. Interfaces 2015, 7, 3335−3341

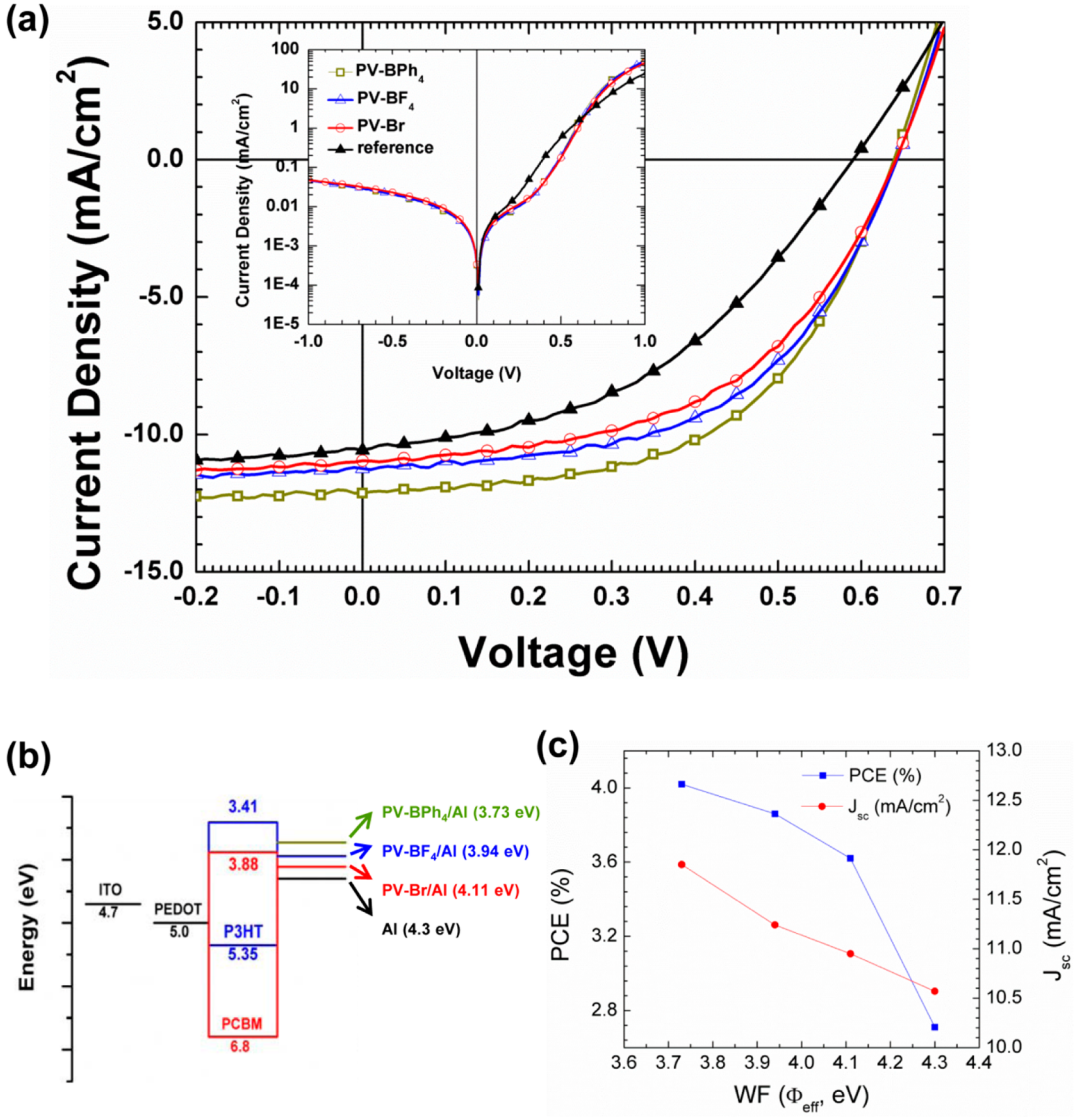

Figure 4. (a) Current density–voltage curves of PSCs under AM 1.5G simulated illumination with an intensity of 100 mW/cm^2 (inset: under dark conditions) with PV-BPh$_4$ (open square), PV-BF$_4$ (open triangle), PV-Br (open circle), and reference (filled triangle), (b) energy level diagram of materials in this study and schematic representation of the work function modification of the cathode by the thin layer of PV-X, and (c) the relationship between the PCE and J_{sc} of each device vs the WF of the Al cathode covered with PV-X.

Table 1. Summary of Photovoltaic Parameters of PSCs Estimated from the Device with the Best PCE Value[a]

	V_{oc} (V)	J_{sc} (mA/cm^2)	FF (%)	PCE (%)	R_s (Ω cm^2)	R_p (kΩ cm^2)
reference	0.59 (0.58 ± 0.01)	10.57 (10.18 ± 0.28)	43.4 (44.4 ± 1.0)	2.71 (2.63 ± 0.12)	5.1	18.3
PV-Br	0.64 (0.63 ± 0.01)	10.95 (10.55 ± 0.25)	51.6 (50.5 ± 1.4)	3.62 (3.41 ± 0.13)	3.1	21.7
PV-BF$_4$	0.64 (0.64 ± 0.01)	11.24 (11.08 ± 0.28)	53.7 (51.8 ± 2.1)	3.86 (3.67 ± 0.13)	2.8	23.9
PV-BPh$_4$	0.64 (0.63 ± 0.01)	11.85 (11.28 ± 0.43)	53.0 (53.0 ± 0.8)	4.02 (3.82 ± 0.13)	3.7	24.2

[a]The averages of the photovoltaic parameters for 10 devices with PV-X of each device are given in parentheses along with the mean variation.

BPh$_4$ are 3.63, 3.86, and 4.02%, respectively, which are dramatically improved over that of the reference device. It should also be noticed that with an increase in the size of the CA in the PV derivatives, the PCE gradually increased. The PCE change, in addition to the J_{sc} values showing good correlation with the change in the WF of the cathode (Figure 4(c)), indicates a typical transition from a Schottky to an Ohmic contact. Generally, a large Schottky barrier impedes the facile injection/collection of electrons at the organic (or polymer) semiconductor/Al interface. Thus, Ohmic contact by the reduction of the Schottky barrier at the interfaces is required to obtain a high J_{sc}.[34,35] Therefore, the most efficient injection/collection of electrons is expected in the device with the PV-BPh$_4$ thin film as the cathode buffer layer.

The current density–voltage curve under dark conditions (inset of Figure 4(a)) provides information about the series resistance (R_s) and the parallel resistance (R_p), which were calculated from the inverse slope near the high current regime and the slope near the lower current region in the dark current density–voltage curves, respectively.[36] Compared to the

DOI: 10.1021/am5082606
ACS Appl. Mater. Interfaces 2015, 7, 3335–3341

reference device (Table 1), the devices with the thin layer of PV derivatives showed smaller R_s and larger FF values, indicating the formation of an Ohmic contact at the cathode interfaces. The R_p values of the device with PV derivatives are also noticeably larger than those of the device without PV derivatives. The R_s and R_p values also reflect the contact properties between the active layer and the cathode. Thus, the property of improved contact at the cathode interface by the thin layer of PV derivatives is another reason for the improved performance of the device. As a result, the PSC with the thin layer of PV-BPh_4 showed the highest PCE (4.02%) with a V_{oc} of 0.64 V, J_{sc} of 11.85 mA/cm^2, and FF of 53.0%. In addition, the incident photon conversion efficiency (IPCE) spectra (see Figure S1 in the Supporting Information) of the devices correlated very well with the J_{sc} change of the devices.

To further investigate the electron injection property of the device with PV derivatives with different types of CAs, we fabricated electron-only devices based on PCBM with the structure ITO/PCBM (~75 nm)/with or without PV-X (~5 nm)/Al (110 nm). According to an energy band diagram under flat band conditions (inset of Figure 5), the energy barriers at

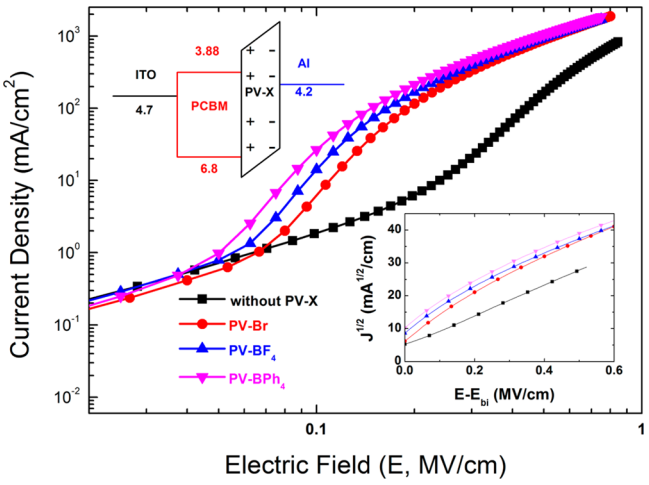

Figure 5. Current density–electric field curves of electron-only devices with a structure of ITO/PCBM/with or without PV-X/Al (E, applied electric filed; E_{bi}, built-in electric field).

the anode and cathode interface were 2.1 and 0.32 eV, respectively. Thus, electrons will be major charge carriers in the device under forward bias. As shown in Figure 5, the turn-on electric field (E_{on}) of the device without PV was 0.21 MV/cm, which is dramatically higher than those of the devices with PV-X (0.07 MV/cm for PV-Br, 0.06 MV/cm for PV-BF_4, and 0.05 MV/cm for PV-BPh_4). This is due to the fact that the electron injection barrier is reduced by the reduction of the Φ_{eff} of Al, which is dependent on the size of the CA. Space-charge-limited current (SCLC) measurements can be used to estimate the charge carrier mobility. Above the built-in electric field (inset of Figure 5), the current density and electric field exhibited a quadratic relationship. This is characteristic of SCLC, which can be described by the Mott–Gurney law

$$J = \frac{9}{8}\varepsilon_0\varepsilon_r\mu_e\frac{E^2}{L}$$

where J is the current density, μ_e is the electron mobility, E is the electric field, $\varepsilon_0\varepsilon_r$ is the PCBM permittivity, and L is the PCBM thickness. Using ε_r = 3.9,[37] we find that the current density and electric field relationship of the device are well described by the Mott–Gurney law. The μ_e of the device without PV-X was 4.63 × 10^{-2} cm^2 V^{-1} s^{-1}, which is quite reasonable.[37] The μ_e values for the device were 5.49 × 10^{-2} cm^2 V^{-1} s^{-1} with PV-Br, 6.54 × 10^{-2} cm^2 V^{-1} s^{-1} with PV-BF_4, and 7.08 × 10^{-2} cm^2 V^{-1} s^{-1} with PV-BPh_4, which are slightly higher than that of the device without PV-X (μ_e = 4.63 × 10^{-2} cm^2 V^{-1} s^{-1}), indicating that the thin layer of PVs does not significantly affect the electron mobility of the devices. The magnitude of the current density of the devices with PV-X is also noticeably higher than that of the device without PV-X, indicating that contact resistance at the cathode is reduced by the thin layer of PV-X.

CONCLUSION

PV derivatives with differing CAs, such as Br^-, BF_4^-, and BPh_4^-, have been demonstrated to function as a cathode buffer layer for PSCs to modify electron injection/collection ability at cathode interfaces. The performance of the PSCs was dependent on the size of the CA (i.e., dipole moment of PV-X). Increased PCE resulted from enhancement of J_{sc}, FF, and V_{oc} simultaneously. We found that the electron injection/collection barrier was dependent on the size of the CA because larger CAs lead to a larger reduction of the work function. The turn-on electric field (E_{on}) of the electron-only device without PV was significantly higher than that of the devices with PV-X. This is also coincident with a decrease in the Schottky barrier at the cathode interface. As a result, the performance of PSCs with PV-BPh_4, which is the largest CA used in this study, showed the best PCE of 4.02% among the devices with PV derivatives. This study provides a very simple and facile strategy relative to structural refinement by complicated syntheses.

ASSOCIATED CONTENT

Supporting Information

IPCE spectrum of PSCs. This material is available free of charge via the Internet at http://pubs.acs.org.

AUTHOR INFORMATION

Corresponding Author

*E-mail: jkim@pknu.ac.kr.

Notes

The authors declare no competing financial interest.

ACKNOWLEDGMENTS

This research was supported by the Basic Science Research Program through the National Research Foundation (NRF) of Korea funded by the Ministry of Education (2014055822).

REFERENCES

(1) Yu, G.; Gao, J.; Hummelen, J. C.; Wudl, F.; Heeger, A. J. Polymer Photovoltaic Cells: Enhanced Efficiencies via a Network of Internal Donor-Acceptor Heterojunctions. *Science* **1995**, *270*, 1789–1791.

(2) Huynh, W. U.; Dittmer, J. J.; Alivisatos, A. P. Hybrid Nanorod-Polymer Solar Cells. *Science* **2002**, *295*, 2425–2427.

(3) Gunes, S.; Neugebauer, H.; Sariciftci, N. S. Conjugated Polymer-Based Organic Solar Cells. *Chem. Rev.* **2007**, *107*, 1324–1338.

(4) Choi, H.; Park, J. S.; Jeong, E.; Kim, G. W.; Lee, B. R.; Kim, S. O.; Song, M. H.; Woo, H. Y.; Kim, J. Y. Combination of Titanium Oxide and a Conjugated Polyelectrolyte for High-Performance Inverted-Type Organic Optoelectronic Devices. *Adv. Mater. (Weinheim, Ger.)* **2011**, *23*, 2759–2763.

DOI: 10.1021/am5082606
ACS Appl. Mater. Interfaces 2015, 7, 3335–3341

(5) Oh, S. H.; Na, S. I.; Jo, J.; Lim, B.; Vak, D.; Kim, D. Y. Water-Soluble Polyfluorenes as an Interfacial Layer Leading to Cathode-Independent High Performance of Organic Solar Cells. *Adv. Funct. Mater.* **2010**, *20*, 1977−1983.
(6) Ma, W.; Iyer, P. K.; Gong, X.; Kiu, B.; Moses, D.; Bazan, G. C.; Heeger, A. J. Water/Methanol-Soluble Conjugated Copolymer as an Electron-Transport Layer in Polymer Light-Emitting Diodes. *Adv. Mater. (Weinheim, Ger.)* **2005**, *17*, 274−277.
(7) Na, S. I.; Oh, S. H.; Kim, S. S.; Kim, D. Y. Efficient Organic Solar Cells with Polyfluorene Derivatives as a Cathode Interfacial Layer. *Org. Electron.* **2009**, *10*, 496−500.
(8) Jin, Y.; Bazan, G. C.; Heeger, A. J.; Kim, J. Y.; Lee, K. Improved Electron Injection in Polymer Light-Emitting Diodes Using Anionic Conjugated Polyelectrolyte. *Appl. Phys. Lett.* **2008**, *93*, 123304-1−123304-3.
(9) Zhu, X.; Xie, Y.; Li, X.; Qiao, X.; Wang, L.; Tu, G. Anionic Conjugated Polyelectrolyte−Wetting Properties with an Emission Layer and Free Ion Migration When Serving as a Cathode Interface Layer in Polymer Light Emitting Diodes (PLEDs). *J. Mater. Chem.* **2012**, *22*, 15490−15494.
(10) Fang, J.; Wallikewitz, B. H.; Gao, F.; Tu, G.; Muller, C.; Pace, G.; Friend, R. H.; Huck, W. T. S. Conjugated Zwitterionic Polyelectrolyte as the Charge Injection Layer for High-Performance Polymer Light-Emitting Diodes. *J. Am. Chem. Soc.* **2011**, *133*, 683−685.
(11) Min, C.; Shi, C.; Zhang, W.; Jiu, T.; Chen, J.; Ma, D.; Fang, J. A Small-Molecule Zwitterionic Electrolyte Without a π-Delocalized Unit as a Charge-Injection Layer for High-Performance PLEDs. *Angew. Chem., Int. Ed.* **2013**, *52*, 3417−3420.
(12) Huang, F.; Zhang, Y.; Liu, M. S.; Jen, A. K. Y. Electron-Rich Alcohol-Soluble Neutral Conjugated Polymers as Highly Efficient Electron-Injecting Materials for Polymer Light-Emitting Diodes. *Adv. Funct. Mater.* **2009**, *19*, 2457−2466.
(13) Wu, H.; Huang, F.; Mo, Y.; Yang, W.; Wang, D.; Peng, J.; Cao, Y. Efficient Electron Injection from a Bilayer Cathode Consisting of Aluminum and Alcohol-/Water-Soluble Conjugated Polymer. *Adv. Mater. (Weinheim, Ger.)* **2004**, *16*, 1826−1830.
(14) Jo, M. Y.; Ha, Y. E.; Kim, J. H. Polyviologen Derivatives as an Interfacial Layer in Polymer Solar Cells. *Sol. Energy Mater. Sol. Cells* **2012**, *107*, 1−8.
(15) Jo, M. Y.; Ha, Y. E.; Kim, J. H. Interfacial Layer Material Derived from Dialkylviologen and Sol−Gel Chemistry for Polymer Solar Cells. *Org. Electron.* **2013**, *14*, 995−1001.
(16) Lim, G. E.; Ha, Y. E.; Jo, M. Y.; Park, J.; Kang, Y. C.; Kim, J. H. Nonconjugated Anionic Polyelectrolyte as an Interfacial Layer for the Organic Optoelectronic Devices. *ACS Appl. Mater. Interfaces* **2013**, *5*, 6508−6513.
(17) Wang, H.; Zhang, W.; Xu, C.; Bi, X.; Chen, B.; Yang, S. Efficiency Enhancement of Polymer Solar Cells by Applying Poly(vinylpyrrolidone) as a Cathode Buffer Layer via Spin Coating or Self-Assembly. *ACS Appl. Mater. Interfaces* **2013**, *5*, 26−34.
(18) Zhang, F.; Ceder, M.; Inganas, O. Enhancing the Photovoltage of Polymer Solar Cells by Using a Modified Cathode. *Adv. Mater. (Weinheim, Ger.)* **2007**, *19*, 1835−1838.
(19) Ha, Y. E.; Lim, G. E.; Jo, M. Y.; Park, J.; Kang, Y. C.; Moon, S. J.; Kim, J. H. Enhancing the Efficiency of Opto-Electronic Devices by the Cathode Modification. *J. Mater. Chem. C* **2004**, *2*, 3820−3825.
(20) Park, J.; Yang, R.; Hoven, C. V.; Garcia, A.; Fischer; Nguyen, D. A. T.; Bazan, G. C.; DeLongchamp, D. M. Structural Characterization of Conjugated Polyelectrolyte Electron Transport Layers by NEXAFS Spectroscopy. *Adv. Mater. (Weinheim, Ger.)* **2008**, *20*, 2491−2496.
(21) Seo, J. W.; Yang, R.; Brzezinski, J. Z.; Walker, B.; Bazan, G. C.; Nguyen, T. Q. Electronic Properties at Gold/Conjugated-Polyelectrolyte Interfaces. *Adv. Mater. (Weinheim, Ger.)* **2009**, *21*, 1006−1011.
(22) Seo, J. H.; Nguyen, T. Q. Electronic Properties of Conjugated Polyelectrolyte Thin Films. *J. Am. Chem. Soc.* **2008**, *130*, 10042−10043.
(23) Garcia, A.; Yang, R.; Jin, Y.; Walker, B.; Nguyen, T.-Q. Structure-Function Relationships of Conjugated Polyelectrolyte Electron Injection Layers in Polymer Light Emitting Diodes. *Appl. Phys. Lett.* **2007**, *91*, 153502-1−153502-3.
(24) Yang, R.; Wu, H.; Cao, Y.; Bazan, G. C. Control of Cationic Conjugated Polymer Performance in Light Emitting Diodes by Choice of Counterion. *J. Am. Chem. Soc.* **2006**, *128*, 14422−14423.
(25) Chang, Y. M.; Zhu, R.; Richard, E.; Chen, C. C.; Li, G.; Yang, Y. Electrostatic Self-Assembly Conjugated Polyelectrolyte-Surfactant Complex as an Interlayer for High Performance Polymer Solar Cells. *Adv. Funct. Mater.* **2012**, *22*, 3284−3289.
(26) Lee, B. H.; Jung, I. H.; Woo, H. Y.; Shim, H. K.; Kim, G.; Lee, K. Multi-Charged Conjugated Polyelectrolytes as a Versatile Work Function Modifier for Organic Electronic Devices. *Adv. Funct. Mater.* **2014**, *24*, 1100−1108.
(27) Seo, J. H.; Jin, Y.; Brzezinski, J. Z.; Walker, B.; Nguyen, T.-Q. Exciton Binding Energies in Conjugated Polyelectrolyte Films. *ChemPhysChem* **2009**, *10*, 1023−1027.
(28) ChemSpider Search and Share Chemistry Home Page. http://www.chemicalize.org (accessed Oct 24, 2014).
(29) Na, S. I.; Kim, T. S.; Oh, S. H.; Kim, J.; Kim, S. S.; Kim, D. Y. Enhanced Performance of Inverted Polymer Solar Cells with Cathode Interfacial Tuning via Water-Soluble Polyfluorenes. *Appl. Phys. Lett.* **2010**, *97*, 223305-1−223305-3.
(30) Park, Y.; Choong, V.; Gao, Y.; Hsieh, B. R.; Tang, C. W. Work Function of Indium Tin Oxide Transparent Conductor Measured by Photoelectron Spectroscopy. *Appl. Phys. Lett.* **1996**, *68*, 2699−2701.
(31) Sze, S. M. *Physics of Semiconductor Devices*, 2nd ed.; Wiley-Interscience: New York, 1981; p 222.
(32) Waldauf, C.; Scharber, M. C.; Schilinsky, P.; Hauch, J. A.; Brabec, C. J. Physics of Organic Bulk Heterojunction Devices for Photovoltaic Applications. *J. Appl. Phys.* **2006**, *99*, 104503.
(33) He, C.; Zhong, C.; Wu, H.; Yang, R.; Tang, W.; Huang, F.; Bazan, G. C.; Cao, Y. Origin of the Enhanced Open-Circuit Voltage in Polymer Solar Cells via Interfacial Modification Using Conjugated Polyelectrolytes. *J. Mater. Chem.* **2010**, *20*, 2617−2622.
(34) Blom, P. W. M.; Mihailetchi, V. D.; Koster, L. J. A.; Markov, D. E. Device Physics of Polymer:Fullerene Bulk Heterojunction Solar Cells. *Adv. Mater. (Weinheim, Ger.)* **2007**, *19*, 1551−1566.
(35) Yip, H. L.; Hau, S. K.; Baek, N. S.; Ma, H. Polymer Solar Cells that Use Self-Assembled-Monolayer-Modified ZnO/Metals as Cathodes. *Adv. Mater. (Weinheim, Ger.)* **2008**, *20*, 2376−2382.
(36) Xue, J.; Uchida, S.; Rand, B. P.; Forrest, S. R. 4.2% Efficient Organic Photovoltaic Cells with Low Series Resistances. *Appl. Phys. Lett.* **2004**, *84*, 3013−3015.
(37) Mihailetchi, V. D.; van Duren, J. K.; Blom, P. W. M.; Hummelen, J. C.; Janssen, R. A. J.; Kroon, J. M.; Rispens, M. T.; Verhees, W. J.; Wienk, M. M. Electron Transport in a Methanofullerene. *Adv. Funct. Mater.* **2003**, *13*, 43−46.

DOI: 10.1021/am5082606
ACS Appl. Mater. Interfaces 2015, 7, 3335−3341